The 1/f-like behavior of neural field spectra are a natural consequence of noise driven brain dynamics

Mark A. Kramer
Department of Mathematics and Statistics, and Center for Systems Neuroscience
Boston University, Boston MA, 02214

Catherine J. Chu
Department of Neurology
Massachusetts General Hospital and Harvard Medical School, Boston MA, 02114

ABSTRACT

Consistent observations across recording modalities, experiments, and neural systems find neural field spectra with 1/f-like scaling, eliciting many alternative theories to explain this universal phenomenon. We propose a general dynamical system with stochastic drive and minimal assumptions to show how correlated and uncorrelated noise generate 1/f-like spectra consistent with *in vivo* observations, without requiring a specific biological mechanism or collective critical behavior.

INTRODUCTION

Transient oscillations are a prominent feature of macroscopic neural field activity [1], linked to brain function [2] and dysfunction [3], [4]. Oscillations appear as narrowband increases in the spectrum above an aperiodic background in which the power P decreases proportional to the frequency f raised to an exponent β: $P \propto f^{\beta}$. Sophisticated methods [5]–[7] support estimation of the 1/f-like, scale-free [8] or power-law [9] behavior of neural field spectra. Changes in β, the aperiodic exponent, have been investigated in many domains, including sleep [10]–[13], aging [14]–[16], and disease [17]–[19]. While many factors impact estimation of the aperiodic exponent (e.g., the frequency range analyzed [20], [21]), values of the exponent reported at higher frequencies (>20 Hz) typically range between -4 and -2 (Table 1).

The universal observation of 1/f-like neural field spectra with a restricted range of aperiodic exponents across different recording modalities, experiments, and neural systems suggests a common generative mechanism. However, many complex, specific mechanisms have been identified to generate this phenomenon. These include excitatory/inhibitory balance [22], low-pass frequency filtering by dendrites [23] or the extracellular medium [24], nonideal resistive components in the cell membrane [25], stochastic firing of neurons convolved with an exponential relaxation process [24], [26], [27], stochastic synaptic conductances [28], stochastically driven damped oscillators with different relaxation rates [29], local homogenous connectivity [30], combinations of many transient oscillations at different frequencies and amplitudes [31], or network mechanisms linking slower rhythms to broad neuronal recruitment and therefore larger amplitude field potentials [23]. Theoretically, scale-free phenomena – with 1/f-like behavior – have been linked to fractal properties [32], critical transitions [9], [33], and self-organized criticality [34], [35]. How these proposed biological and mathematical mechanisms contribute – separately or combined – to the range of aperiodic exponents observed across diverse neural field spectra remains unclear.

Here we demonstrate how, in general, a dynamical system with stochastic drive generates 1/f-like behavior at higher frequencies in neural field spectra. We show that two noise terms – representing correlated and uncorrelated noise inputs – produce the range of aperiodic exponents observed *in vivo*. We illustrate these general results in two specific models of neural activity at different spatial scales. We propose that the range of aperiodic exponents observed *in vivo* is expected in general for dynamical systems with stochastic drive, and not the result of a specific biological mechanism or tuning to collective critical behavior.

RESULTS

As a general model of neural activity, we consider the two-dimensional dynamical system:

$$\frac{dX}{dt} = f(X,Y) + \epsilon_X$$
$$\frac{dY}{dt} = g(X,Y) + \epsilon_Y \,, \tag{1}$$

where X is an observable quantity (e.g., the voltage recorded in the EEG or LFP), Y represents a second variable impacting the observable dynamics (e.g., a transmembrane current), f and g are nonlinear functions, and ϵ_X and ϵ_Y are noise terms (Gaussian distributed with mean 0 and variances σ_X^2 and σ_Y^2, respectively). The unspecified model (1) is general and therefore broadly consistent with diverse models of neural activity; we first consider the dynamics of the general model (1). In what follows, we illustrate these general results using specific model choices for the variables (X,Y) and functions (f,g).

We assume an equilibrium exists in the model so that $\left(\frac{dX}{dt},\frac{dY}{dt}\right) = (0,0)$ at $(X,Y) = (X_0,Y_0)$. Near this equilibrium, the dynamics of the nonlinear system (1) can be approximated by the corresponding linear system,

$$\frac{d\bar{X}}{dt} = \left(\frac{\partial f}{\partial X}\bigg|_{X_0,Y_0}\right)\bar{X} + \left(\frac{\partial f}{\partial Y}\bigg|_{X_0,Y_0}\right)\bar{Y} + \epsilon_X$$
$$\frac{d\bar{Y}}{dt} = \left(\frac{\partial g}{\partial X}\bigg|_{X_0,Y_0}\right)\bar{X} + \left(\frac{\partial g}{\partial Y}\bigg|_{X_0,Y_0}\right)\bar{Y} + \epsilon_Y \,, \tag{2}$$

where $(\bar{X},\bar{Y})$ represent small deviations from the equilibrium (X_0,Y_0), and we evaluate the partial derivatives of the nonlinear functions f,g at the equilibrium (X_0,Y_0) [36], [37]. To simplify notation, we express the system (2) as

$$\frac{d}{dt}\begin{pmatrix}\bar{X}\\ \bar{Y}\end{pmatrix} = \boldsymbol{A}\begin{pmatrix}\bar{X}\\ \bar{Y}\end{pmatrix} + \boldsymbol{B}\begin{pmatrix}\xi_x\\ \xi_y\end{pmatrix}, \tag{3}$$

where $\boldsymbol{A} = \begin{pmatrix}a & b\\ c & d\end{pmatrix}$, $\boldsymbol{B} = \begin{pmatrix}\alpha & 0\\ 0 & 1\end{pmatrix}$, and the (ξ_x,ξ_y) represent noise terms (Gaussian distributed with mean 0 and variances σ_X^2 and σ_Y^2, respectively). The parameters in $\boldsymbol{A}$ determine the local behavior of the nonlinear system (1) near the equilibrium (X_0,Y_0). We assume that $\boldsymbol{A}$ satisfies the conditions required for the linear system (3) to accurately approximate the dynamics of the nonlinear system (1) near the equilibrium (i.e., we assume $\boldsymbol{A}$ has no eigenvalues with zero real part and the equilibrium is hyperbolic [36], [37]).

For the linear system (3), the cross-spectral matrix can be obtained from the expression [38]–[40],

$$\boldsymbol{S}[\omega] = \frac{1}{2\,\pi}\,(\boldsymbol{A} + i\omega\boldsymbol{I})^{-1}\,(\boldsymbol{B}\,\boldsymbol{B}^T)(\boldsymbol{A}^T - i\omega\boldsymbol{I})^{-1}\,, \tag{4}$$

where $\boldsymbol{A}$ is real, $\boldsymbol{I}$ is the identity matrix, $i = \sqrt{-1}$, and $\omega = 2\pi f$ is the frequency. Evaluating the cross-spectral matrix at the parameters utilized here, the spectrum of the observable variable X is,

$$S_{XX}[\omega] = \frac{1}{2\,\pi}\,\frac{b^2 + \alpha^2(d^2+\omega^2)}{(b\,c - a\,d)^2 + (a^2 + 2\,b\,c + d^2)\omega^2 + \omega^4}\,. \tag{5}$$

We now consider how the spectrum of the observable variable ($S_{XX}[\omega]$) behaves at high frequencies (ω larger than any frequency associated with a natural rhythm of the linear system in (3)). Without stochastic drive to the variable X (i.e., with $\alpha = 0$) and with $b \neq 0$ (i.e., with the latent variable Y driving changes in the observable variable X),

$$S_{XX}[\omega] \propto \frac{b^2}{\omega^4}\,,$$

so that the aperiodic exponent $\beta = -4$ at high frequencies. Alternatively, with stochastic drive to the observable variable X (i.e., with $\alpha \neq 0$),

$$S_{XX}[\omega] \propto \frac{\omega^2}{\omega^4} \propto \frac{1}{\omega^2}$$

so that the aperiodic exponent $\beta = -2$ at high frequencies.

To summarize, we consider a general, two-dimensional nonlinear dynamical system with stochastic drive (1). We assume an equilibrium exists in this system with dynamics well-approximated by the linearized system (2). Near this equilibrium, the dynamics produce aperiodic exponents between -4 and -2 at high frequencies, consistent with the values observed *in vivo*. The value of the aperiodic exponent depends on the relative noise in the two variables; when noise in the observable variable X dominates, the aperiodic exponent ≈ -2, while when the noise in the latent variable Y dominates, the aperiodic exponent ≈ -4.

In what follows, we illustrate these results in two example models of neural activity, in which we choose the nonlinear functions f and g in model (1).

Example 1: The Wilson-Cowan model

We first consider the Wilson-Cowan equations as a model of neural population activity [41]. The equations describe the interacting dynamics of an excitatory (E) and inhibitory (I) neural population,

$$\begin{aligned} \tau_e \frac{dE}{dt} &= -E + (k_e - r_e\, E)\, \mathcal{S}_e[c_1 E - c_2 I + P] + \epsilon_E \\ \tau_i \frac{dI}{dt} &= -I + (k_i - r_i\, I)\ \ \mathcal{S}_i[c_3 E - c_4 I + Q] + \epsilon_I\,, \end{aligned} \tag{6}$$

where $\mathcal{S}$ is the sigmoid function

$$\mathcal{S}_k[x] = \frac{1}{1 + \exp\big(-a_k\,(x - \theta_k)\big)} - \frac{1}{1 + \exp(a_k\,\theta_k)}\,.$$

We choose the parameters to produce damped oscillatory behavior (see Figure 10 of [41] and the caption of Figure 1 for the parameter values used here). With these parameters, we find an equilibrium of the model (6),

$$(E_0, I_0) \approx (0.1511, 0.1585)\,.$$

The linearized system near this equilibrium is approximately,

$$\begin{aligned} \frac{d\bar{E}}{dt} &= \ 1.482\,\bar{V} - 2.660\,\bar{I} + \epsilon_E \\ \frac{d\bar{I}}{dt} &= \ 3.963\,\bar{V} - 1.981\,\bar{I} + \ \epsilon_I\,, \end{aligned}$$

and the equilibrium is hyperbolic, with eigenvalues $-0.250 \pm 2.75\,i$.

According to the general theory, we expect the nonlinear system (6) near the equilibrium (E_0, I_0) to produce spectra with aperiodic exponents $-4 \leq \beta \leq -2$, depending on the values of the stochastic drives (ϵ_E, ϵ_I). To show this, we simulate the nonlinear system (6) and estimate the spectrum of the excitatory variable E with fixed inhibitory noise ($\sigma_I = 0.1$) and variable excitatory noise ($0 \leq \sigma_E \leq 0.3$). In agreement with the general theory (Figure 1), as the excitatory noise increases, the aperiodic exponent increases from near $\beta \approx -4$ when $\sigma_E = 0$ to $\beta \approx -2$ when $\sigma_E = 0.3$.

We conclude that this nonlinear model of neural population activity (6) produces aperiodic exponents consistent with the range of values observed *in vivo*. In this model, the value of the aperiodic exponent depends on the relative noise in the observable variable E and latent variable I. When noise in the inhibitory population dominates, the aperiodic exponent approaches -4; when noise in the excitatory population dominates, the aperiodic exponent approaches -2.

Example 2: A Hodgkin-Huxley type model

We next consider a reduced Hodgkin-Huxley type model [36], [42]. We choose this model to simulate the subthreshold dynamics of a single neuron, in contrast to the neural population dynamics simulated in the previous example. The model equations describe the dynamics of an observable voltage (V) and a latent membrane current (M),

$$\begin{aligned} \frac{dV}{dt} &= I_0 + g_M M(E_M - V) + \epsilon_V \\ \frac{dM}{dt} &= \alpha_M[V](1-M) - \beta_M[V]M + \epsilon_M \,. \end{aligned} \tag{7}$$

In the first equation, three terms drive the voltage dynamics: a constant input current (I_0), a dynamic membrane current ($g_M M(E_M - V)$), and voltage noise (ϵ_V, Gaussian distributed with mean 0 and variance σ_V^2). In the second equation, the dynamics of the latent membrane current depend on forward ($\alpha_M[V]$) and backward ($\beta_M[V]$) rate functions,

$$\alpha_M[V] = \frac{0.02}{1 + \exp(\frac{-V-20}{5})}$$

$$\beta_M[V] = 0.01 \exp(\frac{-V-43}{18}) \,.$$

We choose these functions to simulate a muscarinic receptor suppressed potassium current (M-current, see Table A2 of [43]) [44], [45]. We omit other membrane currents (e.g., fast sodium and potassium currents) to focus on the subthreshold membrane dynamics without action potential generation. A stochastic drive also impacts the membrane current dynamics (ϵ_M, Gaussian distributed with mean 0 and variance σ_M^2).

Choosing the model parameters $I_0 = 1,\ g_M = 4$, and $E_M = -95$, we find an equilibrium of the model (7) at

$$(V_0, M_0) \approx (-48.15, 0.00534) \,.$$

The linearized system near this equilibrium is approximately,

$$\begin{aligned} \frac{d\bar{V}}{dt} &= -0.0213\,\bar{V} - 187.38\,\bar{M} + \epsilon_V \\ \frac{d\bar{M}}{dt} &= 0.0000181\,\bar{V} - 0.0134\,\bar{M} + \epsilon_M \,, \end{aligned}$$

and the equilibrium is hyperbolic with eigenvalues $-0.0174 \pm 0.0581\,i$.

Consistent with the general theory, we expect this nonlinear Hodgkin-Huxley type model (7) to produce spectra with aperiodic exponents $-4 \le \beta \le -2$, depending on the values of the stochastic drives (ϵ_V, ϵ_M). To show this, we simulate the Hodgkin-Huxley type model (7) and estimate the spectrum of the voltage variable V with fixed current noise ($\sigma_M = 0.01$) and variable voltage noise ($0 \le \sigma_V \le 30$). In agreement with the general theory, as the voltage noise increases, the aperiodic exponent increases from near $\beta \approx -4$ when $\sigma_V = 0$ to $\beta \approx -2$ when $\sigma_V = 30$.

We conclude that this nonlinear model of single neuron subthreshold dynamics (7) produces aperiodic exponents consistent with the range of values observed *in vivo*. In agreement with the general theory, the value of the aperiodic exponent depends on the relative noise in the observable voltage variable and latent current variable. In this case, when noise in the membrane current dominates, the aperiodic exponent approaches -4; when noise in the voltage dominates, the aperiodic exponent approaches -2.

DISCUSSION

A universal feature of neural field potential spectra is 1/f-like scaling. To produce this power-law, many generative mechanisms have been proposed with diverse biological implementations and interpretations. Here, we consider an unspecified nonlinear dynamical system with stochastic drive. We show that dynamics near a (hyperbolic) equilibrium in this general model produce aperiodic exponents between -4 and -2, consistent with the range of values reported *in vivo* for higher frequencies (e.g., >20 Hz). We illustrate these results in two biophysical models representing neural activity at different spatial scales. We conclude that the range of aperiodic exponents observed across recording modalities, experiments, and neural systems is a natural consequence of a noise driven dynamical system.

Under the general framework considered here, the range of aperiodic exponents reflects different types of noise. We note that the observable dynamics (e.g., variable X in (1)) depend on two types of noise: directly on the stochastic drive to the observable variable, and indirectly on the stochastic drive to the latent variable. The latent dynamics introduce correlations in the uncorrelated latent noise process before this noise reaches the observable dynamics. Therefore, the observable dynamics depend on both uncorrelated and correlated noise inputs, and we may interpret the aperiodic exponent in terms of these different types of noise; an aperiodic exponent near $\beta = -4$ indicates correlated noise inputs dominate the high frequency observable dynamics, while $\beta = -2$ indicates uncorrelated noise dominates the high frequency observable dynamics. These general results are independent of a specific biophysical mechanism, and a biophysical interpretation of the relationship between different types of noise and the aperiodic exponent depends on the specific model choice.

We consider a two-dimensional dynamical system, with one observable variable and one latent variable. While models of brain activity may be higher dimensional, we note that observed large-scale neural dynamics often evolve on low-dimensional stable manifolds [46]–[48]. While we expect the results derived here will hold in higher dimensions, the analytic expressions become much more difficult to interpret for dimensions greater than two.

Some observations report aperiodic exponents greater than -2 (i.e., $\beta > -2$). Experimental factors, such as measurement noise which flattens the spectrum and shifts β towards 0, might contribute to these observations. In addition, analysis factors may impact reported results. For example, the frequency range considered varies widely across studies (see discussion of fitting ranges in [21]). In general, larger aperiodic exponents (more negative β) occur at higher frequencies [24], [49]–[51], although not always [52]. In the framework considered here, the result $-4 \leq \beta \leq -2$ holds in the high frequency limit, when the measured frequency exceeds any natural frequency of the neural population. We expect analyzing lower frequency bands (e.g., below the natural frequency), or analyzing the low and high frequency bands after accounting for the broadband peak, will increase the exponent in this model. While potentially useful, the aperiodic exponent reported in lower frequency bands is more difficult to interpret. To assess low frequency rhythms requires long durations of data, which increases the chance of non-stationarities. Artifacts (e.g., slow drifts) and analysis choices (e.g., whether to subtract the signal mean) also impact the low frequency power. Finally, while power-law features at low frequencies may reflect the same power-law features at high frequencies, these different phenomena unlikely reflect the same neural mechanisms.

Many well-supported observations of power-laws appear in neuroscience (e.g., avalanches of population voltage discharges [53], amplitudes of narrowband oscillations [54]). Here, we consider one type of power-law: the 1/f-like neural field spectrum and a general, noise-driven dynamical system. Under this general model, the aperiodic exponent represents two types of noise, without requiring a sophisticated biological or dynamical mechanism. The range of aperiodic exponents $-4 \leq \beta \leq -2$ requires no specific mechanism; these aperiodic exponents simply represent the expected dynamics near an equilibrium in a nonlinear dynamical system driven by noise. The generality of the model is consistent with the universality of 1/f-like field spectra, reflecting a basic feature of

spontaneous neural noise beyond neural oscillations. However, this simplicity may also limit the computational utility of this mechanism and the role of the aperiodic exponent in measuring neural computations. We conclude that the most parsimonious explanation of 1/f-like neural field spectra is just (two types) of noise.

Table 1: Example aperiodic exponents for human voltage spectra reported in the literature*. The mean value of the aperiodic exponent (β) reported in the reference listed in column Ref. Additional details include the year of study, recording modality, number of subjects n and additional subject information, frequency range analyzed, and experimental condition. Considering only those studies with minimum frequencies >20 Hz (yellow highlighted rows), the aperiodic exponent has mean -3.1, lower quartile -4, and upper quartile -2.5.*

β	Ref	Year	Recording modality	Frequency	Experimental condition
-0.08	[49]	2019	Scalp EEG (n=5)	20-40 Hz	Anesthesia (Ketamine)
-1.12	[19]	2022	Scalp EEG (n=16, control subjects)	1-40 Hz	Eyes closed
-1.3	[55]	2021	Scalp EEG (n=74, Tourette syndrome)	2-40 Hz	Behavioral experiments
-1.44	[55]	2021	Scalp EEG (n=74, control)	2-40 Hz	Behavioral experiments
-1.48	[19]	2022	Scalp EEG (n=18, stroke patients)	1-40 Hz	Stroke patients
-1.51	[18]	2019	Scalp EEG (n=78, control subjects)	4-50 Hz	Resting state
-1.67	[18]	2019	Scalp EEG (n=76, ADHD subjects)	4-50 Hz	Resting state
-1.84	[10]	2020	Scalp EEG (n=9)	30-45 Hz	Wakefulness
-1.86	[56]	2013	Scalp EEG (n=7, adults)	0.2-30 Hz	Sleep
-1.87	[10]	2020	Scalp EEG (n=14)	30-45 Hz	Resting state
-2.03	[49]	2019	Scalp EEG (n=5)	20-40 Hz	Wakefulness
-2.07	[56]	2013	Scalp EEG (n=15, newborns)	0.2-30 Hz	Sleep
-2.32	[57]	2000	Intracranial EEG (n=5)	0.5-150 Hz	Resting state
-2.33	[12]	2021	Scalp EEG (n=175, T5)	2-48 Hz	NREM sleep
-2.44	[31]	2010	Intracranial EEG (n=5)	1-100 Hz	Wakefulness
-2.48	[49]	2019	Scalp EEG (n=5)	20-40 Hz	Wakefulness
-2.71	[11]	2022	Scalp EEG (n=251)	2-48 Hz	NREM sleep
-2.73	[12]	2021	Scalp EEG (n=175, Fz)	2-48 Hz	NREM sleep
-2.75	[10]	2020	Intracranial EEG (n=12)	30-45 Hz	Wakefulness
-2.87	[31]	2010	Intracranial EEG (n=5)	1-100 Hz	Slow wave sleep
-2.99	[10]	2020	Intracranial EEG (n=10)	30-45 Hz	Wakefulness
-3.1	[10]	2020	Scalp EEG (n=9)	30-45 Hz	Anesthesia
-3.13	[49]	2019	Scalp EEG (n=5)	20-40 Hz	Wakefulness
-3.46	[10]	2020	Scalp EEG (n=14)	30-45 Hz	N3 Sleep
-3.59	[49]	2019	Scalp EEG (n=5)	20-40 Hz	Anesthesia (Xenon)
-3.67	[10]	2020	Scalp EEG (n=14)	30-45 Hz	N2 Sleep
-3.69	[10]	2020	Intracranial EEG (n=10)	30-45 Hz	N3 Sleep
-4	[27]	2009	Intracranial EEG (n=20)	80-500 Hz	Behavioral experiments
-4.15	[10]	2020	Intracranial EEG (n=10)	30-45 Hz	REM sleep
-4.34	[10]	2020	Intracranial EEG (n=12)	30-45 Hz	Anesthesia
-4.36	[49]	2019	Scalp EEG (n=5)	20-40 Hz	Anesthesia (Propofol)
-4.73	[10]	2020	Scalp EEG (n=14)	30-45 Hz	REM sleep

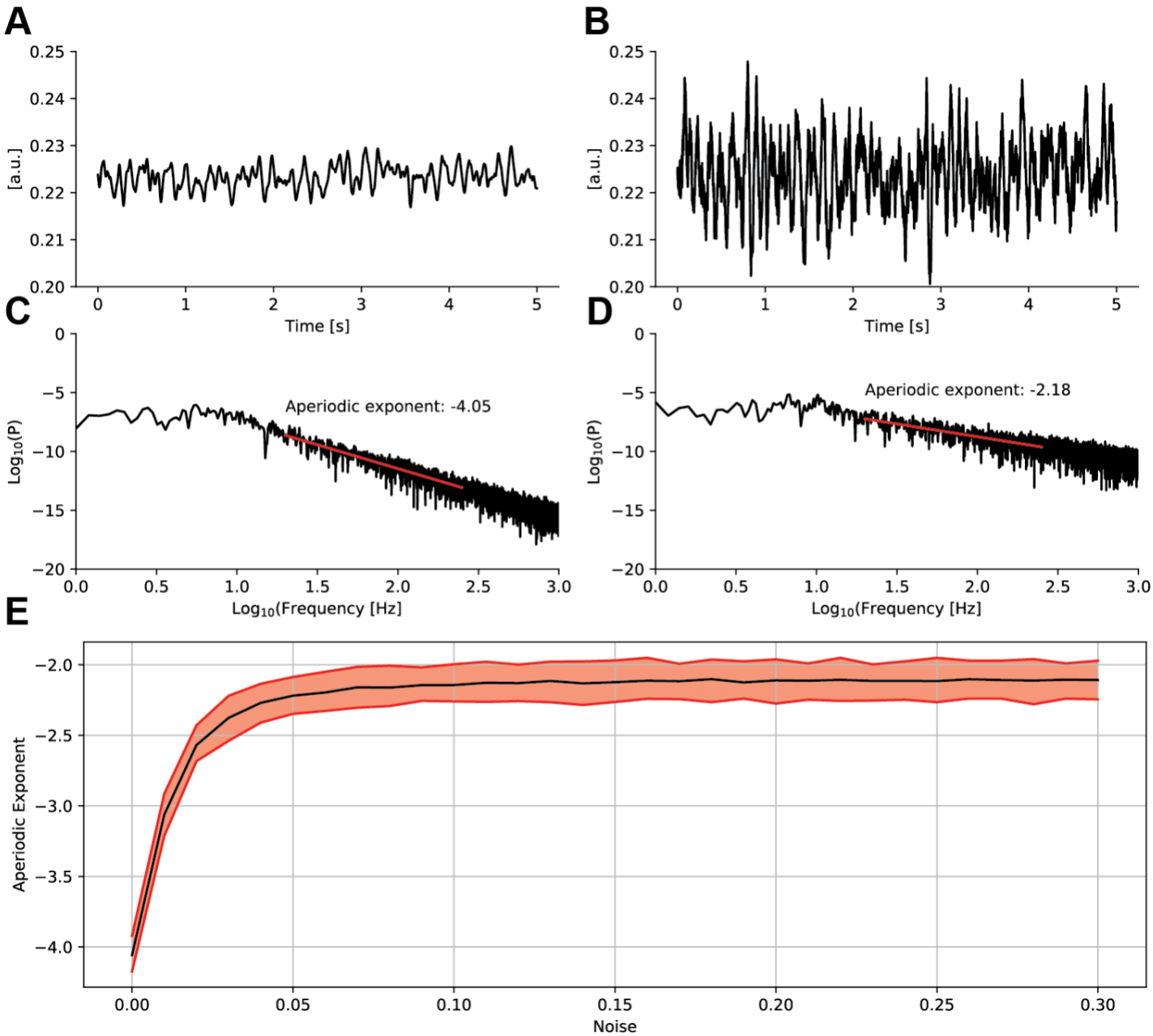

Figure 1: In the Wilson-Cowan model, the aperiodic exponent increases from approximately -4 to -2 with the excitatory noise. (A,B) *Example excitatory population time series when (A) the excitatory noise is 0 (i.e., $\epsilon_E = 0$), or (B) the excitatory noise is non-zero (i.e., $\sigma_E = 0.2$).* ***(C,D)*** *The corresponding spectra (black) and linear fits (red, 20 Hz to 250 Hz) for the time series in (A,B).* ***(E)*** *Estimates of the aperiodic exponent for increasing values of excitatory noise. Black (red) indicates mean (standard deviation) of estimates across 100 simulations. In all simulations, the inhibitory noise ($\sigma_I = 0.1$) is fixed. We use the model parameters: $c_1 = 15, c_2 = 15, c_3 = 15, c_4 = 7, a_e = 1, \theta_e = 2, a_i = 2, \theta_i = 2.5, \tau_e = 50, \tau_i = 50, r_e = 1, r_i = 1, k_e = 1, k_i = 1, P = 1.25, Q = 0$. Code to simulate the model and create this figure is available at https://github.com/Mark-Kramer/Aperiodic-Exponent-Model.*

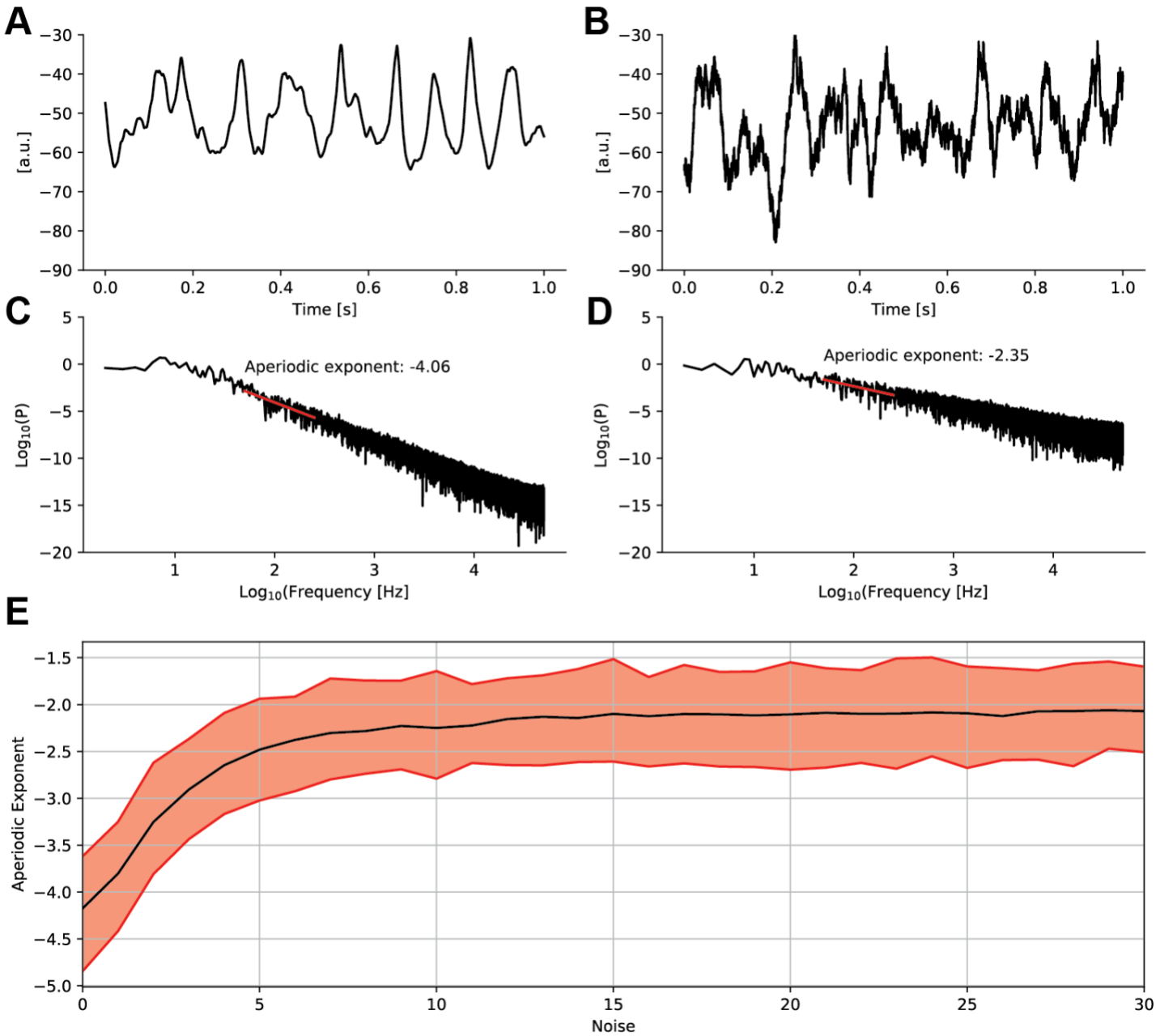

Figure 2: In a Hodgkin-Huxley type model, the aperiodic exponent increases from approximately -4 to -2 with the voltage noise. (A,B) *Example voltage time series when (A) the voltage noise is 0 (i.e., $\epsilon_V = 0$), or (B) the voltage noise is non-zero (i.e., $\sigma_V = 20$).* ***(C,D)*** *The corresponding spectra (black) and linear fits (red, 50 Hz to 250 Hz) for the time series in (A,B).* ***(E)*** *Estimates of the aperiodic exponent for increasing values of voltage noise. Black (red) indicates mean (standard deviation) of estimates across 100 simulations. In all simulations, the current noise ($\sigma_M = 0.01$) is fixed. Code to simulate the model and create this figure is available at https://github.com/Mark-Kramer/Aperiodic-Exponent-Model*

MATERIALS AND METHODS

Estimation of the aperiodic exponent β from time series data

To estimate the aperiodic exponent β, we first compute the spectrum in the standard way. To a simulated voltage time series (V_t) with sampling interval Δ and duration T, we subtract the mean, apply a Hanning taper, compute the Fourier transform (V_f), and multiply by the complex conjugate (V_f^*):

$$P = \frac{2\,\Delta^2}{T}\, V_f\, V_f^* \,.$$

We note that the square of the Fourier coefficients is essential for consistent interpretation of the aperiodic exponent across studies; omitting the square is a common mistake identified in previous work (see discussion in [58]). For frequencies f, we fit a linear model to the logarithm base 10 of the spectrum ($\log_{10} P$) with predictor logarithm base 10 of the frequency ($\log_{10} f$),

$$\log_{10} P = c + \beta \log_{10} f \,,$$

where β is the estimate of the aperiodic exponent. Code to compute the spectrum and estimate the aperiodic exponent is available at https://github.com/Mark-Kramer/Aperiodic-Exponent-Model.

ACKNOWLEDGEMENTS

The authors would like to thank Konstantinos Spiliopoulos and Uri Eden for recommendations regarding the analysis of stochastic differential equations. The authors were supported in part by NSF #1451384, NIH R01NS110669, and R01NS119483.

REFERENCES

[1] G. Buzsaki, *Rhythms of the Brain*. Oxford University Press, 2011.

[2] G. Buzsaki and A. Draguhn, “Neuronal Oscillations in Cortical Networks,” *Science*, vol. 304, no. 5679, pp. 1926–1929, Jun. 2004, doi: 10.1126/science.1099745.

[3] P. J. Uhlhaas and W. Singer, “Neuronal Dynamics and Neuropsychiatric Disorders: Toward a Translational Paradigm for Dysfunctional Large-Scale Networks,” *NEURON*, vol. 75, no. 6, pp. 963–980, Sep. 2012.

[4] Gibbs and Lennox, “Epilepsy: a paroxysmal cerebral dysrhythmia,” *Epilepsy & behavior : E&B*, vol. 3, no. 4, pp. 395–401, Aug. 2002.

[5] T. Donoghue *et al.*, “Parameterizing neural power spectra into periodic and aperiodic components,” *Nat Neurosci*, vol. 23, no. 12, pp. 1655–1665, Dec. 2020, doi: 10.1038/s41593-020-00744-x.

[6] H. Wen and Z. Liu, “Separating Fractal and Oscillatory Components in the Power Spectrum of Neurophysiological Signal,” *Brain Topogr*, vol. 29, no. 1, pp. 13–26, Jan. 2016, doi: 10.1007/s10548-015-0448-0.

[7] L. E. Wilson, J. da Silva Castanheira, and S. Baillet, “Time-resolved parameterization of aperiodic and periodic brain activity,” *eLife*, vol. 11, p. e77348, Sep. 2022, doi: 10.7554/eLife.77348.

[8] B. J. He, “Scale-free brain activity: past, present, and future,” *Trends in Cognitive Sciences*, vol. 18, no. 9, pp. 480–487, Sep. 2014, doi: 10.1016/j.tics.2014.04.003.

[9] M. Newman, “Power laws, Pareto distributions and Zipf’s law,” *Contemporary Physics*, vol. 46, no. 5, pp. 323–351, Sep. 2005, doi: 10.1080/00107510500052444.

[10] J. D. Lendner *et al.*, “An electrophysiological marker of arousal level in humans,” *eLife*, vol. 9, p. e55092, Jul. 2020, doi: 10.7554/eLife.55092.

[11] C. G. Horváth *et al.*, “Overnight dynamics in scale-free and oscillatory spectral parameters of NREM sleep EEG,” *Sci Rep*, vol. 12, no. 1, Art. no. 1, Nov. 2022, doi: 10.1038/s41598-022-23033-y.

[12] R. Bódizs *et al.*, “A set of composite, non-redundant EEG measures of NREM sleep based on the power law scaling of the Fourier spectrum,” *Sci Rep*, vol. 11, no. 1, p. 2041, Jan. 2021, doi: 10.1038/s41598-021-81230-7.

[13] W. J. Freeman and J. Zhai, “Simulated power spectral density (PSD) of background electrocorticogram (ECoG),” *Cogn Neurodyn*, vol. 3, no. 1, pp. 97–103, Mar. 2009, doi: 10.1007/s11571-008-9064-y.

[14] N. Schaworonkow and B. Voytek, “Longitudinal changes in aperiodic and periodic activity in electrophysiological recordings in the first seven months of life,” *Developmental Cognitive Neuroscience*, vol. 47, p. 100895, Feb. 2021, doi: 10.1016/j.dcn.2020.100895.

[15] B. Voytek *et al.*, “Age-Related Changes in 1/f Neural Electrophysiological Noise,” *J. Neurosci.*, vol. 35, no. 38, pp. 13257–13265, Sep. 2015, doi: 10.1523/JNEUROSCI.2332-14.2015.

[16] E. Cesnaite *et al.*, “Alterations in rhythmic and non-rhythmic resting-state EEG activity and their link to cognition in older age,” *NeuroImage*, vol. 268, p. 119810, Mar. 2023, doi: 10.1016/j.neuroimage.2022.119810.

[17] T. Numan *et al.*, “Regional healthy brain activity, glioma occurrence and symptomatology,” *Brain*, vol. 145, no. 10, pp. 3654–3665, Oct. 2022, doi: 10.1093/brain/awac180.

[18] M. M. Robertson, S. Furlong, B. Voytek, T. Donoghue, C. A. Boettiger, and M. A. Sheridan, “EEG power spectral slope differs by ADHD status and stimulant medication exposure in early childhood,” *Journal of Neurophysiology*, vol. 122, no. 6, pp. 2427–2437, Dec. 2019, doi: 10.1152/jn.00388.2019.

[19] J. Lanzone *et al.*, “EEG spectral exponent as a synthetic index for the longitudinal assessment of stroke recovery,” *Clinical Neurophysiology*, vol. 137, pp. 92–101, May 2022, doi: 10.1016/j.clinph.2022.02.022.

[20] M. P. H. Stumpf and M. A. Porter, “Critical Truths About Power Laws,” *Science*, vol. 335, no. 6069, pp. 665–666, Feb. 2012, doi: 10.1126/science.1216142.

[21] M. Gerster *et al.*, “Separating Neural Oscillations from Aperiodic 1/f Activity: Challenges and Recommendations,” *Neuroinform*, vol. 20, no. 4, pp. 991–1012, Oct. 2022, doi: 10.1007/s12021-022-09581-8.

[22] R. Gao, E. J. Peterson, and B. Voytek, “Inferring synaptic excitation/inhibition balance from field potentials,” *NeuroImage*, vol. 158, pp. 70–78, Sep. 2017, doi: 10.1016/j.neuroimage.2017.06.078.

[23] G. Buzsáki, C. Anastassiou, and C. Koch, “The origin of extracellular fields and currents — EEG, ECoG, LFP and spikes,” *Nature Reviews Neuroscience*, vol. 13, no. 6, pp. 407–420, Jan. 2012, doi: 10.1038/nrn3241.

[24] C. Bédard, H. Kröger, and A. Destexhe, “Does the 1/f frequency scaling of brain signals reflect self-organized critical states?,” *Physical Review Letters*, vol. 97, no. 11, p. 118102, Sep. 2006.
[25] C. Bédard and A. Destexhe, “A Modified Cable Formalism for Modeling Neuronal Membranes at High Frequencies,” *Biophysical Journal*, vol. 94, no. 4, pp. 1133–1143, Feb. 2008, doi: 10.1529/biophysj.107.113571.
[26] J. Milstein, F. Mormann, I. Fried, and C. Koch, “Neuronal shot noise and Brownian 1/f2 behavior in the local field potential,” *PLoS ONE*, vol. 4, no. 2, p. e4338, 2009.
[27] K. Miller, L. Sorensen, J. Ojemann, and M. den Nijs, “Power-Law Scaling in the Brain Surface Electric Potential,” *PLoS Comput Biol*, vol. 5, no. 12, p. e1000609 EP, Dec. 2009, doi: 10.1371/journal.pcbi.1000609.
[28] M. Rudolph, J. G. Pelletier, D. Paré, and A. Destexhe, “Characterization of Synaptic Conductances and Integrative Properties During Electrically Induced EEG-Activated States in Neocortical Neurons In Vivo,” *Journal of Neurophysiology*, vol. 94, no. 4, pp. 2805–2821, Oct. 2005, doi: 10.1152/jn.01313.2004.
[29] R. Evertz, D. G. Hicks, and D. T. J. Liley, “Alpha blocking and 1/fβ spectral scaling in resting EEG can be accounted for by a sum of damped alpha band oscillatory processes,” *PLOS Computational Biology*, vol. 18, no. 4, p. e1010012, Apr. 2022, doi: 10.1371/journal.pcbi.1010012.
[30] V. K. Jirsa, “Neural field dynamics with local and global connectivity and time delay,” *Philos Trans A Math Phys Eng Sci*, vol. 367, no. 1891, pp. 1131–1143, Mar. 2009, doi: 10.1098/rsta.2008.0260.
[31] B. J. He, J. M. Zempel, A. Z. Snyder, and M. E. Raichle, “The temporal structures and functional significance of scale-free brain activity,” *NEURON*, vol. 66, no. 3, pp. 353–369, May 2010, doi: 10.1016/j.neuron.2010.04.020.
[32] W. S. Pritchard, “The Brain in Fractal Time: 1/F-Like Power Spectrum Scaling of the Human Electroencephalogram,” *International Journal of Neuroscience*, vol. 66, no. 1–2, pp. 119–129, Jan. 1992, doi: 10.3109/00207459208999796.
[33] J. O’Byrne and K. Jerbi, “How critical is brain criticality?,” *Trends in Neurosciences*, vol. 45, no. 11, pp. 820–837, Nov. 2022, doi: 10.1016/j.tins.2022.08.007.
[34] P. Bak, C. Tang, and K. Wiesenfeld, “Self-organized criticality: An explanation of the 1/ *f* noise,” *Phys. Rev. Lett.*, vol. 59, no. 4, pp. 381–384, Jul. 1987, doi: 10.1103/PhysRevLett.59.381.
[35] L. Cocchi, L. L. Gollo, A. Zalesky, and M. Breakspear, “Criticality in the brain: A synthesis of neurobiology, models and cognition,” *Progress in Neurobiology*, vol. 158, pp. 132–152, Nov. 2017, doi: 10.1016/j.pneurobio.2017.07.002.
[36] Izhikevich, E, *Dynamical Systems in Neuroscience*. MIT Press, 2007.
[37] Guckenheimer, John and Holmes, Philip, *Nonlinear Oscillations, Dynamical Systems, and Bifurcations of Vector Fields*. Springer-Verlag, 1983.
[38] P. J. Thomas and B. Lindner, “Phase descriptions of a multidimensional Ornstein-Uhlenbeck process,” *Phys. Rev. E*, vol. 99, no. 6, p. 062221, Jun. 2019, doi: 10.1103/PhysRevE.99.062221.
[39] R. Kleeman, “Spectral Analysis of Multidimensional Stochastic Geophysical Models with an Application to Decadal ENSO Variability,” *Journal of the Atmospheric Sciences*, vol. 68, no. 1, pp. 13–25, Jan. 2011, doi: 10.1175/2010JAS3546.1.
[40] Gardiner, C, *Handbook of Stochastic Methods*. Springer-Verlag, 2004.
[41] H. R. Wilson and J. D. Cowan, “Excitatory and Inhibitory Interactions in Localized Populations of Model Neurons,” *Biophysical Journal*, vol. 12, no. 1, pp. 1–24, Jan. 1972, doi: 10.1016/S0006-3495(72)86068-5.
[42] A. L. Hodgkin and A. F. Huxley, “A quantitative description of membrane current and its application to conduction and excitation in nerve,” *The Journal of Physiology*, vol. 117, no. 4, pp. 500–544, 1952, doi: 10.1113/jphysiol.1952.sp004764.
[43] R. D. Traub, E. H. Buhl, T. Gloveli, and M. A. Whittington, “Fast Rhythmic Bursting Can Be Induced in Layer 2/3 Cortical Neurons by Enhancing Persistent Na+ Conductance or by Blocking BK Channels,” *Journal of Neurophysiology*, vol. 89, no. 2, pp. 909–921, Feb. 2003, doi: 10.1152/jn.00573.2002.
[44] M. A. Kramer, A. K. Roopun, L. M. Carracedo, R. D. Traub, M. A. Whittington, and N. J. Kopell, “Rhythm Generation through Period Concatenation in Rat Somatosensory Cortex,” *PLOS Computational Biology*, vol. 4, no. 9, p. e1000169, Sep. 2008, doi: 10.1371/journal.pcbi.1000169.
[45] N. Kopell, M. A. Whittington, and M. A. Kramer, “Neuronal assembly dynamics in the beta1 frequency range permits short-term memory,” *PNAS*, vol. 108, no. 9, pp. 3779–3784, Mar. 2011, doi: 10.1073/pnas.1019676108.
[46] J. P. Cunningham and B. M. Yu, “Dimensionality reduction for large-scale neural recordings,” *Nature Neuroscience*, vol. 17, no. 11, pp. 1500–1509, Nov. 2014, doi: 10.1038/nn.3776.

[47] R. Chaudhuri, B. Gerçek, B. Pandey, A. Peyrache, and I. Fiete, “The intrinsic attractor manifold and population dynamics of a canonical cognitive circuit across waking and sleep,” *Nat Neurosci*, vol. 22, no. 9, Art. no. 9, Sep. 2019, doi: 10.1038/s41593-019-0460-x.
[48] J. M. Shine *et al.*, “The Low-Dimensional Neural Architecture of Cognitive Complexity Is Related to Activity in Medial Thalamic Nuclei,” *Neuron*, vol. 104, no. 5, pp. 849-855.e3, Dec. 2019, doi: 10.1016/j.neuron.2019.09.002.
[49] M. A. Colombo *et al.*, “The spectral exponent of the resting EEG indexes the presence of consciousness during unresponsiveness induced by propofol, xenon, and ketamine,” *NeuroImage*, vol. 189, pp. 631–644, Apr. 2019, doi: 10.1016/j.neuroimage.2019.01.024.
[50] F. S. Racz *et al.*, “Separating scale-free and oscillatory components of neural activity in schizophrenia,” *Brain and Behavior*, vol. 11, no. 5, p. e02047, 2021, doi: 10.1002/brb3.2047.
[51] A. Ibarra Chaoul and M. Siegel, “Cortical correlation structure of aperiodic neuronal population activity,” *NeuroImage*, vol. 245, p. 118672, Dec. 2021, doi: 10.1016/j.neuroimage.2021.118672.
[52] R. Chaudhuri, B. J. He, and X.-J. Wang, “Random Recurrent Networks Near Criticality Capture the Broadband Power Distribution of Human ECoG Dynamics,” *Cerebral Cortex*, vol. 28, no. 10, pp. 3610–3622, Oct. 2018, doi: 10.1093/cercor/bhx233.
[53] J. M. Beggs and D. Plenz, “Neuronal Avalanches in Neocortical Circuits,” *J. Neurosci.*, vol. 23, no. 35, pp. 11167–11177, Dec. 2003, doi: 10.1523/JNEUROSCI.23-35-11167.2003.
[54] K. Linkenkaer-Hansen, V. V. Nikouline, J. M. Palva, and R. J. Ilmoniemi, “Long-Range Temporal Correlations and Scaling Behavior in Human Brain Oscillations,” *J. Neurosci.*, vol. 21, no. 4, pp. 1370–1377, Feb. 2001, doi: 10.1523/JNEUROSCI.21-04-01370.2001.
[55] N. Adelhöfer *et al.*, “Increased scale-free and aperiodic neural activity during sensorimotor integration—a novel facet in Tourette syndrome,” *Brain Communications*, vol. 3, no. 4, p. fcab250, Oct. 2021, doi: 10.1093/braincomms/fcab250.
[56] P. Fransson, M. Metsäranta, M. Blennow, U. Åden, H. Lagercrantz, and S. Vanhatalo, “Early Development of Spatial Patterns of Power-Law Frequency Scaling in fMRI Resting-State and EEG Data in the Newborn Brain,” *Cerebral Cortex*, vol. 23, no. 3, pp. 638–646, Mar. 2013, doi: 10.1093/cercor/bhs047.
[57] W. J. Freeman, L. J. Rogers, M. D. Holmes, and D. L. Silbergeld, “Spatial spectral analysis of human electrocorticograms including the alpha and gamma bands,” *Journal of Neuroscience Methods*, vol. 95, no. 2, pp. 111–121, Feb. 2000, doi: 10.1016/S0165-0270(99)00160-0.
[58] E. Milotti, “1/f noise: a pedagogical review.” arXiv, Apr. 12, 2002. Accessed: Oct. 25, 2022. [Online]. Available: http://arxiv.org/abs/physics/0204033